# 光吸收性 粉体粒子에 對한 레이저散亂光 粉体粒度測定機의 反應 特性

# Response of Laser Light Active Scattering Aerosol Spectrometer to Light-Absorbing Aerosol Particulates

鄭 仁 碩 · 趙 慶 國*
In Seuck Jeung · Kyung Kook Cho

抄 錄

Berglund-Liu 振動方式 單分散 粉体粒子 發生機(Berglund-Liu vibrating orifice monodisperse aerosol generator)에 依하여 製作한 單分散 光吸收性 標準粉体粒子를 使用하여 레이저 散亂光 粉体粒度測定機 (Knollenberg active scattering aerosol spectrometer)의 反應特性을 調査하였다.

實驗結果, 機器의 反應特性은 Mie 散亂理論에 依하여 計算한 理論値와 매우 잘 一致하며 特히 光吸收性 粉体粒子는 光通過性 粉体粒子가 多意的인 特性을 나타내는 것에 反하여 거의 單調增加하는 一意的인 特性을 가지고 있으며 光吸收性 粉体粒子의 反應特性이 製作者의 較正値에 가까운 結果를 나타내었다.

## Introduction

Optical single particle counting is a technique of aerosol analysis in its ability to show particle size distribution data. Optical single particle counting is based on the measurement of light scattering from individual particles, then particle size or size distribution data is determined from sizing the intensity of light scattering corresponding to each particle sampled into optical counting instrument. But for chemically and physically different aerosols, light scattering intensity is dependent not only on particle size but also on the other properties of the aerosol, i.e., particle shape and complex index of refraction, also on lens geometry of counter optics and photodetector spectral characteristics.

Pinnick and his collaborators (Pinnick and Auvermann, 1979; Pinnick and Rosen, 1979; Pinnick et al., 1981; Garvey and Pinnick, 1982) presented wide observation of response characteristics of optical light scattering particle counter, typically on the "Knollenberg" light scattering particle counters (followed after the developer, R.G. Knollenberg, now they are manufactured by Particle Measuring Systems, Inc. (Boulder, Colorado)) to have better and more adequate understanding of their response characteristics and limitations. These understandings are necessary to obtain proper results excluding possible errors in measurements made with them.

It is also true that usually optical light scattering particle counter are calibrated with

*正會員, 서울大學校 航空工學科

ideal nonabsorbing spherical aerosols, except some examples of india ink aerosol by Whitby and Vomela (1967) or nigrosin dye aerosol by Pinnick and Auvermann (1979). But, in many practical cases, non-ideal light absorbing irregular particles are to be measured, for example, in-cylinder particle measurement from a diesel engine (Du and Kittelson, 1983) and explosion dust particles measurement (Pinnick et al., 1983).

In this paper, we attempt to obtain the response characteristics of Knollenberg ASAS-300X active scattering aerosol spectrometer particle counter to several light-absorbing aerosols. It is highly desirable to generate known monodisperse light-absorbing aerosols with different light-absorbing coefficients, to investigate the counter response behavior to light-absorbing aerosols. Next section will be given to explain the general description for aerosols generation technique of used three different monodisperse light-absorbing aerosols. In the third section, general description of optical system and related opto-electronic system in Knollenberg ASAS-300X particle counter is given. And the brief explanation for the theoretical response calculation using Mie theory for a spherical particle scattering in standing wave radiation will be followed. Finally, comparison of theoretical response and experimental results for the ASAS-300X particle counter to light-absorbing aerosols are discussed.

## Generation of monodisperse light-absorbing aerosols

The aerosol generation system known as the vibrating orifice monodisperse aerosol generator (commercially available from TSI, Inc. (St. Paul, Minnesota)) is quite similar to that described by Berglund and Liu (1973). The system, shown in figure 1, is composed of a droplet generation and dispersion unit and an aerosol dilution and transport unit. The electrical charge occurred during the droplet generation process is neutralized by means of a 10 mCi Krypton-85 radioactive neutralizer source, which is placed along the inside wall of the vertical drying column as an integral part of the generator. More details of the structure, performance, and basic operation of this generator can be found from Berglund and Liu (1973).

In these experiments, a 10 $\mu$m diameter orifice was used in the case of aerosol generation whose diameter is lower than 3 $\mu$m. The liquid flow rate was set at 0.0557 ml/min. A 15 $\mu$m diameter orifice was also used to generate aerosols large than 3 $\mu$m diameter. The liquid flow rate was set at 0.1395 ml/min in this case. The vibrating frequency was varied from 30 KHz to 250 KHz maximum.

The diameter of the aerosol produced by the generator can be calculated by the equation.

$$D = (6QC/\pi f)^{1/3} \qquad (1)$$

where, Q is the liquid flow rate, C is the volumetric concentration of flomaster ink, methylene blue, and india ink in the solution, and f is the vibrating frequency.

Here, we used three kinds of light-absorbing aerosols, i.e., flomaster ink as the weak light-absorbing aerosol, methylene blue as the moderate light-absorbing aerosol, and india ink as the strong light-absorbing aerosol. Methylene blue and india ink were dissolved and diluted in a 50:50 liquid mixture of isopropyl alcohol and distilled water, and flomaster ink was dissolved and diluted in pure acetone. The physical characteristics

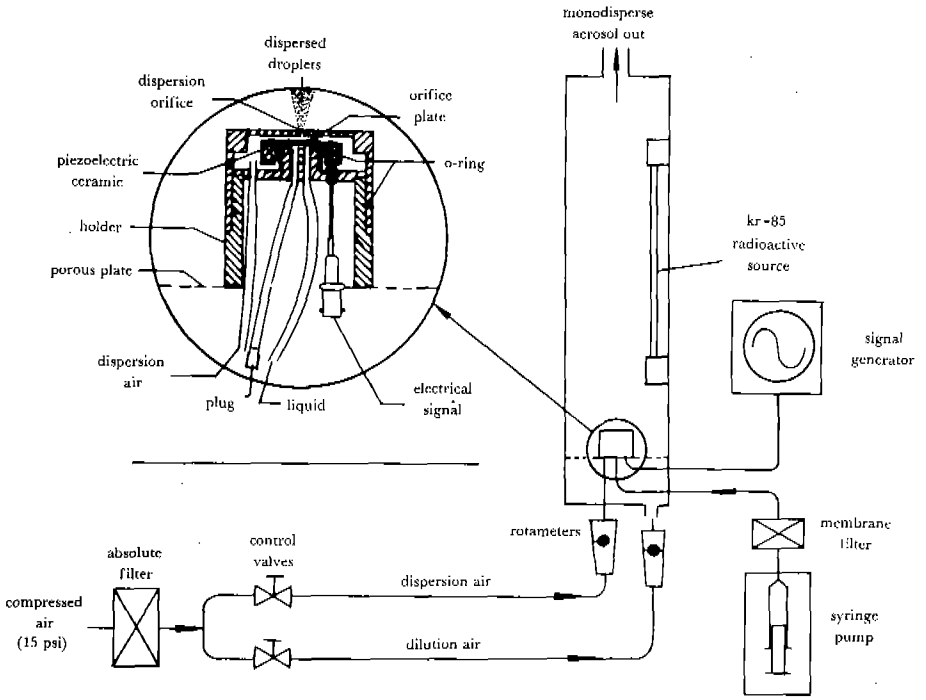


Fig. 1. Schematic diagram of vibrating orifice aerosol generator (VOAG).

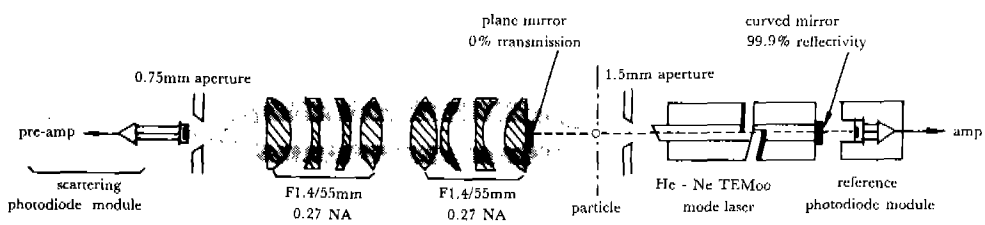


Fig. 2. Schematic diagram of ASAS-300X Knollenberg active scattering aerosol spectrometer particle counter optical system.

of used inks and methylene blue aerosols are shown in table 1. Density of ink aerosol or methylene blue aerosol is assumed to be same as that of solid residual of ink or methylene blue powder measured by an air pycnometer.

The aerosol particles generated by the method described above were collected with an impactor onto a glass microscope slide coated with silicone oil. The diameter of the aerosols on the microscope slide was measured by an optical microscope using a Cooke image splitting eyepiece.

Table 1. Physical characteristics of used aerosols

| aerosol | flomaster ink | methylene blue | india ink |
|---|---|---|---|
| complex index of refraction | 1.65 - 0.069i [a] | 1.57 - 0.17i [b] | 1.95 - 0.66i [c,d] |
| shape | dented | spherical | spherical |
| weight fraction of solid residual | 31.6% | - | 15.8% |
| reference | Pinnick et al. (1973) | Fagan (1982) | Fenn (1976) |

a) measured at $\lambda = 632.8$nm(He-Ne laser light)

b) measured at $\lambda = 655$nm

c) complex index of refraction of india ink is assumed to be that of carbon, as most of solid residual of india ink is carbon black pigment

d) measured at visible wavelength range

## Active scattering aerosol spectrometer particle counter

A schematic of the optical system of the ASAS-300X particle counter from a drawing in the standard manual supplied by manufacturer is shown in figure 2. Its airflow system is aligned to isolate the particle sample stream from critical optical components as well as confine the particle stream to the defined boundaries of the laser beam (to the central 15% of the beam width) in order to provide for uniform illumination of particles. The Gaussian $TEM_{00}$ mode 2 mW He-Ne open-cavity laser (623.8 nm) is used as the particle illumination source. A merit of utilizing the open-cavity laser as the particle illumination source is that the high energy density is available (According to Knollenberg and Luehr (1976), brightness in excess 1000 W/cm$^2$ is attainable.) and permits measurement of small particles down to 0.05 $\mu$m diameter when the photomultiplier tube is used as the photodetector sensor (Knollenberg, 1979). The particle stream is aerodynamically focussed to a 200 $\mu$m diameter particle sample stream surrounded by a filtered sheath airflow.

The scattered light from particles in this defined sample volume is relayed from the object plane by collecting lenses at the angles between 4° and 22° from the direction of forward scattering, then collected to the scattering photodetector module. In the scattering photodetector module, the signals which are derived from the particles that do not pass through the defined boundaries of the laser beam, or defined sample volume, are out-of-focus and electronically rejected by comparing two divided signals from a masked beamsplitter that can derive two signals from the collected scattered light, those are one through signal aperture and the other through masked aperture.

The scattering photodetector module consists of a photodiode detector (EG & G SGD-100A), an amplifier operating in a current-to-voltage converter mode, two programmable operational amplifiers with four internally multiplexed operational amplifier operating at gains compatible with the size ranges selected. The gains for Range 1 and Range 3 relative to Range 0 are 10.046 and 667.7.

The light transmitted out the back curved laser mirror is collected by the reference photodiode detector (EG & G SGD-100A), which provides a signal proportional to the illumination on the particles, so that changes in laser output are thus cancelled when the signal is applied as the reference input of the pulse height analyzer.

## Theoretical response calculations

As described earlier, ASAS-300X uses the intra-cavity standing wave radiation of a hybrid He-Ne laser as a light source, or in other words, particles detected in this counter pass through the standing wave radiation within laser cavity. The intensity of the scattered radiation (or theoretical response) from an individual particle in the standing wave radiation, I, can be calculated by adding the Mie scattering amplitude for each plane wave traveling opposite direction with each other,

$$I = \frac{\pi}{k^2}\int_{\alpha}^{\beta} [\,|S_1(\theta) + S_1(\pi-\theta)|^2 + |S_2(\theta) + S_2(\pi-\theta)|^2\,] \sin\theta \, d\theta \qquad (2)$$

where, $S_1(x, m, \theta)$ and $S_2(x, m, \theta)$ are the

Mie scattering amplitude functions corresponding to light polarized with electric vector perpendicular and parallel to the plane of scattering. The Mie scattering amplitude functions are dependent upon the particle size parameter, $x = kr$ (k; wavenumber, r; particle radius), the complex index of refraction, $m = n + i\varkappa$ (n; real part, $\varkappa$; imaginary part or absorption coefficient), and scattering angle, $\theta$. For the case of ASAS-300X, integration is done from $\alpha = 4^\circ$ to $\beta = 22^\circ$.

This solution is derived under the some assumptions. First, the intensity of the standing wave radiation remains constant even by the presence of the scatterparticles passing through the laser beam. Second, plane waves are in phase as the particle to be measured is always centered at the standing wave anti-nodal point. Practically, the defined sample volume is much larger than half the laser wavelength, so that a particle probably traverses other regions as well as antinodal point. The practical probelems of in-phase and out-of-phase will be discussed briefly later.

## Results and discussion

Voltage threshold limits from manufacturer and theoretical response for polystyrene latex particles ($m = 1.592 - 0i$) are presented in figure 3. Manufacturer's voltage threshold limits are expressed in voltage per particle and normalized to the theoretical results for best least-square-fit to the theoretical response of polystyrene latex particles. The normalization constant employed in least-square-fitting the voltage threshold limits or experimental data to the theoretical response is,

$$1 \text{ volt} = 4.7 \times 10 \text{ cm}^2 \quad \text{or}$$
$$C = 2.1 \times 10 \text{ mV/cm}^2 \qquad (3)$$

and this single normalization constant was used for all experimental results.

It is noted that voltage threshold limits from manufacturer is smoothing the first, second resonances and higher order resonances, which cause misreading of measurement if the manufacturer calibration is used in the region of particle size larger than about 1 $\mu$m diameter, as the instrument response on nonabsorbing aerosols shows many multivalued behavior above the first resonance diameter (where aerosol diameter is comparable to the light wavelength). But, it can be readily seen that all the instrument response is fairly in good agreement with the theoretical predictions, when the smaller particle size than about 1 $\mu$m diameter is concerned. Polystyrene latex particle measurements by Pinnick and Auvermann (1979)

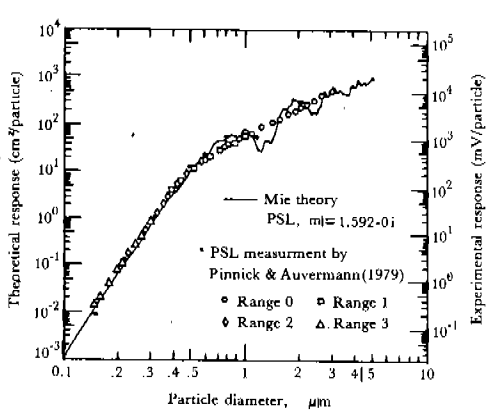


Fig. 3. Comparison of Knollenberg ASAS-300X response; manufacturer's voltage threshold limits for each range and theoretical calculation using Mie scattering for a particle in a standing wave radiation for single polystyrene latex (PSL) nonabsorbing spherical particle. Scale of theoretical response is abitrary and is chosen as a relative scale with dimension of $\text{cm}^2$/particle. Voltage threshold limits have been fit to Mie scattering response using a single normalization constant ($C = 2.1 \times 10 \text{ mV/cm}^2$).

also showed almost exactly same results.

The instrument response of flomaster ink aerosol having weak absorption coefficient is shown in figure 4. The experimental response voltages were determined from the count mean diameter corresponding to peak signal channel reading, the relative gain ratios for each given ranges, and manufacturer's voltage threshold limits provided with the instrument manual shown in figure 3. The error bars for each measurement represent the signal broadening but at least 68% of the signals for these particles have pulse heights falling between the error bars.

First resonance behavior predicted by Mie theoretical calculation was resolved by the experimental results, even though second weak resonance was not appropriately reproduced. Relatively wide broadening of signals of flomaster ink aerosols may be due to the fast drying, resulting flomaster ink aerosol shape to be dented not to be spherical (Whitby and Vomela, 1967), as the solvent used to dissolve flomaster ink was pure acetone.

As seen in figure 4, in the size ranges within the trough of the first resonance region, it can be easily understood that the instrument response should be multivalued, resulting no size classification. It is noticeable that most of all experimental results are fairly in good agreement with the theoretical predictions except multivalued behavior around 1$\mu$m diameter region and signal decreasing above the instrument upper measuring range limit of 3 $\mu$m diameter as observed by Pinnick and Auvermann (1979). This behavior is same tenency with other light-absorbing aerosols which will be discussed later. It is also noticeable that the response voltages of flomaster ink aerosols larger than 2.5 $\mu$m approximately are lower signal levels than manufacturer's voltage threshold limits.

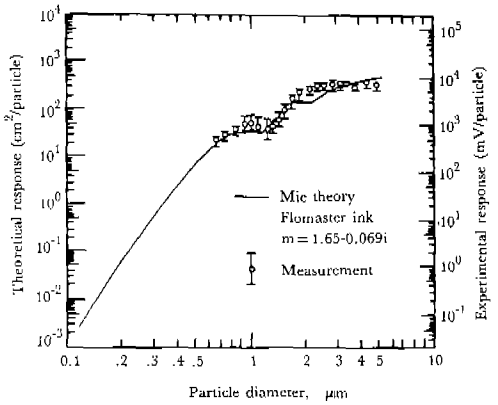


Fig. 4. Comparison of Knollenberg ASAS-300X response for flomaster ink; measured for weak absorbing dented particles and theoretical calculation using Mie scattering for spherical particles of equal cross-sectional area. Other legends are same as in Figure 3.

Response of methylene blue aerosol having moderate absorption coefficient is shown in figure 5. First resonance or higher order resonances can not be easily distinguished, rather behavior of methylene blue aerosol is almost of monotonical behavior differently from the weak absorbing aerosols like flomaster ink aerosols or polystyrene latex aerosols. Notice that signal decreasing

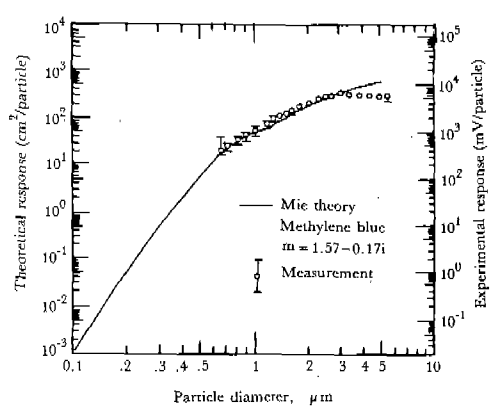


Fig. 5. Comparison of Knollenberg ASAS-300X response for methylene blue; measured response and theoretical calculation using Mie scattering for moderate absorbing spherical particles. Other legends are same as in Figure 3.

above the instrument upper limit is easily recognized as same as the response on flomaster ink aerosols. It is recognized that the signal broadening of smaller particle is rather wider than that of larger particle. This phenomena would be probably due to the impurities in used solvents, as the impurity concentration becomes a considerable order, as highly diluted solutions were used to generate submicron particles.

The instrument response of india ink aerosol having strong absorption coefficient is presented in figure 6. In this case, the complex index of refraction to calculate Mie scattering for india ink was used that of carbon, as we could not find an appropriate value for india ink. This, using the complex index of refraction of carbon instead of that of india ink itself, would be one of reasons that the small deviation between theoretical predictions and DMA (Differential Mobility Analyzer) experimental results for submicron india ink aerosols (below 0.4 $\mu$m approximately) prepared by Liu et al. (1984)

It can be readily understood that the response on this case is almost same result as that of methylene blue aerosol having moderate absorption coefficient and of monotonically varying behavior. It suggests that it has moderate light-absorbing characteristics like methylene blue aerosol ($m = 1.57 - 0.17i$), the instrument response characteristics would fully show the behavior due to the strong light-absorbing aerosols, or in other words, the response characteristics of ASAS-300X to the light-absorbing aerosols is such that it behaviors like explained above if the absorption coefficient is the order of that of methylene blue aerosol (approximately $\kappa = 0.15 - 0.20$).

As indicated earlier, experimental results in this case also show the signal decreasing

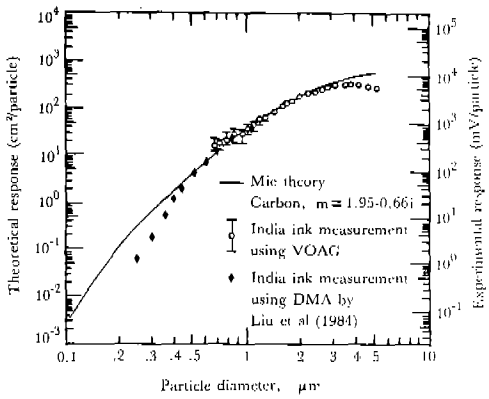


Fig. 6. Comparison of Knollenberg ASAS-300X response for india ink; measured for strong absorbing spherical india ink particles and theoretical calculation using Mie scattering for carbon particle ($m = 1.95-0.66i$). Other legends are same as in Figure 3.

above the instrument upper limit as other cases. This effect seems to be result of particles being large enough to reduce operating laser power. This effect is reported by Schuster and Knollenberg (1972) and Knollenberg (1976). According to their results, the loss fraction of $TEM_{00}$ mode laser is given by

$$Y_{00} = 8a^2/w^2 \qquad (4)$$

where, $Y_{00}$ is the induced loss fraction, a; particle radius, w; spot size of the intensity pattern. If we select the particle radius 1.5 $\mu$m, which is the corresponding size to the instrument upper limit, and spot size 100 $\mu$m, which is corresponding to the sample volume size, then the relative output laser power is approximately 80% of the original unperturbed power according to their experimental result for $TEM_{00}$ mode laser. Another one reason that signal level is decreasing above the instrument upper limit would be due to the phase problem between standing wave and particle position, as particle size is large enough comparing to the wavelength that out-of-phase may be occurred. This effect means that the theoretical Mie calculations

do not hold no longer in the case of out-of-phase between wavefront and particle.

All the theoretical response for polystyrene latex, flomaster ink, methylene blue, carbon particles are summarized with the voltage threshold limits of ASAS-300X particle counter in figure 7. Here, we can see that all the responses of light-absorbing aerosols have lower signal level than manufacturer voltage threshold limits, which can cause lower sizing than the actual size if the manufacturer calibration is directly used. However, the response of light-absorbing aerosols has simple response characteristics that it can be simply corrected from the indicated instrument readings by using simple multiplication factor comparing to the complicated response of nonabsorbing aerosols.

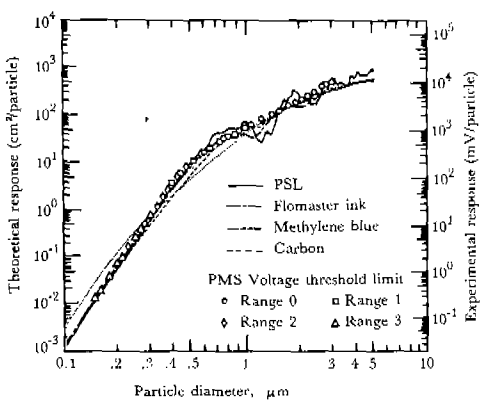


Fig. 7. Comparison of Knollenberg ASAS-300X response; manufacturer's voltage threshold limits and theoretical calculations using Mie sacttering for polystyrene latex (PSL) particles, flomaster ink particles, methylene blue particles, and carbon particles. Other legends are same as in Figure 3.

## Concluding remarks

By this experiments and theoretical Mie scattering calculations, it is found that the response of Knollenberg ASAS-300X particle counter to light-absorbing spherical aerosols is almost of monotonically increasing single-valued behavior comparing to the multivalued behavior of nonabsorbing spherical aerosols, and the instrument response to light absorbing aerosols are better closer to the manufacturer calibration than response to nonabsorbing aerosols, if we consider simple multiplication correction to the manufacturer calibration data. But it is strongly recommened to have a calibration procedure with some appropriate standard aerosols having similar physical and chemical properties with particles in question to be measured actually, as the instrument response is dependent on the aerosol properties as well as particle size, even though the difference between actual calibration and manufacturer calibration would be small.

It is recommended to eliminate unmeasurable or unwanted particles larger than 3 μm diameter by using some treatment like impactor which can cut out the large particles before entering into the instrument, as the instrument response in this range gives incorrect informations.

Finally, it is suggested that these calibration data would be properly applied to the measurement of carbonaceous particles and other strong light-absorbing particles.

## Acknowledgement

Authors gratefully acknowledge Dr. W. Szymanski for his Mie computer calculation for us and his DMA measurement contributions. One of authors (I.-S. Jeung) expresses his appreciation to KOSEF for his financial support to extend his postdoctoral fellowship.

## References

R. N. Berglund and B.Y.H. Liu (1973).

Environmental Science and Technology 7:147-153.

C. J. Du and D.B. Kittelson (1983). SAE technical paper 830243, The Society of Automotive Engineers.

W.G. Eagan (1982). Applied Optics 21:1445-1453.

R.W. Fenn (1976). Optical Properties of Aerosols in Handbook on Aerosols (R. Dennis ed.), Technical Information Center, ERDA, p. 85.

D.M. Garvey and R.G. Pinnick (1982). Submitted to Aerosol Science and Technology.

R.G. Knollenberg and R. Luehr (1976). In Fine Particles (B.Y.H. Liu ed.), Academic Press.

R.G. Knollenberg (1979). In Aerosol Measurement (D.A. Lundgren et al. ed.), University Presses of Florida.

B.Y.H. Liu et al. (1984). Unpublished work.

R.G. Pinnick et al. (1973). Applied Optics 12:37-41.

R.G. Pinnick and J.J. Auvermann (1979). Journal of Aerosol Science 10:55-74.

R.G. Pinnick and J.M. Rosen (1979). Journal of Aerosol Science 10:533-538.

R.G. Pinnick et al. (1981). Journal of Applied Meteorology 20:1049-1057.

R.G. Pinnick et al. (1983). Applied Optics 22:95-102.

B.G. Schuster and R. Knollenberg (1972). Applied Optics 11:1515-1520.

K.T. Whitby and R.A. Vomela (1967). Environmental Science and Technology 1:801-814.